J Neuropathol Exp Neurol
Vol. 75, No. 9, September 2016, pp. 903–916
doi: 10.1093/jnen/nlw065

ORIGINAL ARTICLE

Amyloid-β Precursor Protein Modulates the Sorting of Testican-1 and Contributes to Its Accumulation in Brain Tissue and Cerebrospinal Fluid from Patients with Alzheimer Disease

Alvaro Barrera-Ocampo, PhD, Sönke Arlt, Dr. Med, Jakob Matschke, Dr. Med, Ursula Hartmann, Dr. Med, Berta Puig, PhD, Isidre Ferrer, Dr. Med, PhD, Petra Zürbig, PhD, Markus Glatzel, Dr. Med, Diego Sepulveda-Falla, Dr. Med, and Holger Jahn, Dr. Med

Abstract

The mechanisms leading to amyloid-β (Aβ) accumulation in sporadic Alzheimer disease (AD) are unknown but both increased production or impaired clearance likely contribute to aggregation. To understand the potential roles of the extracellular matrix proteoglycan Testican-1 in the pathophysiology of AD, we used samples from AD patients and controls and an *in vitro* approach. Protein expression analysis showed increased levels of Testican-1 in frontal and temporal cortex of AD patients; histological analysis showed that Testican-1 accumulates and co-aggregates with Aβ plaques in the frontal, temporal and entorhinal cortices of AD patients. Proteomic analysis identified 10 fragments of Testican-1 in cerebrospinal fluid (CSF) from AD patients. HEK293T cells expressing human wild type or mutant Aβ precursor protein (APP) were transfected with Testican-1. The co-expression of both proteins modified the sorting of Testican-1 into the endocytic pathway leading to its transient accumulation in Golgi, which seemed to affect APP processing, as indicated by reduced Aβ40 and Aβ42 levels in APP mutant cells. In conclusion, patient data reflect a clearance impairment that may favor Aβ accumulation in AD brains and our *in vitro* model supports the notion that the interaction between APP and Testican-1 may be a key step in the production and aggregation of Aβ species.

From the Institute of Neuropathology (AB-O, JM, BP, MG, DS-F), Department of Psychiatry and Psychotherapy (SA, HJ), University Medical Center Hamburg-Eppendorf, Hamburg, Germany, Center for Biochemistry, Medical Faculty, University of Cologne, Cologne, Germany (UH), Institute of Neuropathology, Bellvitge University Hospital, CIBERNED, Hospitalet de Llobregat, University of Barcelona, Spain (IF), Mosaiques Diagnostics and Therapeutics AG, Hannover, Germany (PZ), and Department of Pharmaceutical Sciences, Natura Research Group, Faculty of Natural Sciences, ICESI University, Cali, Colombia (AB-O)

Send correspondence to: Diego Sepulveda-Falla, Dr. Med., Institute of Neuropathology, University Medical Center Hamburg-Eppendorf, Martinistr. 52, N27/02.005, 20246 Hamburg, Germany, E-mail: dsepulve@uke.de

This study was funded by grant No. 01EW0909 to MG, IF and HJ by the German Federal Ministry of Education and Research in the frame of the ERA-NET NEURO project "ADtest: Role of proteases and their inhibitors in pathophysiology and diagnosis of Alzheimer Disease". DS-F was supported by this grant and AB-O was supported by a DAAD scholarship

Conflict of interest: The authors declare no conflict of interest.

Supplementary Data can be found at http://www.jnen.oxfordjournals.org.

Key Words: *β*-Amyloid, Alzheimer disease, APP Swedish mutation, Early endosomes, Neuritic plaques, Testican-1.

INTRODUCTION

The accumulation of amyloid-β (Aβ) in the brain is one of the principal processes involved in the pathogenesis of Alzheimer disease (AD). Aβ deposition is a gradual process characterized by the presence of diffuse plaques at early stages of the disease that evolve into neuritic plaques in later stages (1, 2). Aβ aggregation follows a hierarchical pattern showing cortical (including the medial temporal lobe) and hippocampal distribution in the early stages, and in the late phases affecting regions such as the striatum, brainstem and cerebellum (3, 4).

Mutations in *APP*, *PSEN1*, or *PSEN2* genes increase the production of Aβ. However, the mechanisms of Aβ increased production in late-onset sporadic AD are not well understood (5). Some explanations to the accumulation of Aβ include changes in the activity of the enzymes involved in the processing of Aβ precursor protein (APP), i.e. β- and γ-secretases. Additionally, it has been proposed that deficiencies in Aβ clearance may also contribute to the aggregation process. For example, Mawuenyega et al studied the kinetics of Aβ production and clearance using a leucine isotope to label Aβ peptides in AD patients and healthy individuals and found that while the production of Aβ40 and Aβ42 was unaffected, the clearance of the peptides was decreased in AD patients (6).

The idea of clearance impairment in AD is supported by the fact that many other proteins have been found both in amyloid plaques (7), and the CSF of affected individuals (8). Using a proteomic approach we identified over 100 peptides present in CSF of AD patients that differed from those in healthy controls and patients with other neurodegenerative disorders (9). One of the peptides found in that study corresponds to the C-terminal fragment (CTF) of Testican-1, which specifically showed increased levels in AD patients.

Testican-1 is an extracellular matrix proteoglycan coded in humans by the *SPOCK1* gene (10, 11). Testican-1 protein domains are related to neurogenesis and are found in proteins such as adhesion molecules, growth factor binding proteins

and protease inhibitors (12). Testican-1 is highly expressed in the human brain with increased mRNA levels in thalamic and hippocampal neurons (13, 14). It is also expressed in reactive astrocytes after injury and may affect axonal regeneration (15). Previous studies suggested that Testican-1 may play a role in Aβ-mediated pathology due to its ability to modulate proteins like cathepsin-L and matrix metalloproteinase 2, which are involved in the production and degradation of Aβ (16, 17). In addition, other proteoglycans have been found to be associated with amyloid plaques in the brains of AD patients. This interaction seems to enhance the nucleation phase and contribute to the stabilization of the β structure required for fibril formation and Aβ aggregation (18). Based on evidence implicating Testican-1 in the pathophysiology of AD, we evaluated the expression patterns and levels of Testican-1 in brains of AD patients and healthy individuals using tissue microarray (TMA) and Western blot, and performed a proteomic study of CSF samples from AD patients, frontotemporal dementia (FTD), schizophrenia and cognitively healthy individuals. We also investigated the relationship between Testican-1 accumulation and the processing and sorting of APP using an *in vitro* model of AD.

MATERIALS AND METHODS

Ethics Statement

The study was approved by the ethics committee of the "Ärztekammer Hamburg", Germany; all patients and/or their relatives gave written informed consent and all clinical investigations were conducted according to the principles expressed in the Declaration of Helsinki. Furthermore, the University Medical Center Hamburg-Eppendorf has carried out all investigations according to international Good Laboratory Practice and Good Clinical Practice standards.

Patient Characteristics

A summary of the neuropathological and demographic characteristics of the AD and control patients included in the Western blot and TMA experiments is provided in the Tables 1 and 2, respectively. For the proteomic study, patients referred to the memory clinic of the University Medical Center Hamburg-Eppendorf were recruited. All patients were assessed according to the National Institute of Neurological and Communicative Disorders and the Stroke-Alzheimer's Disease and Related Disorders Association criteria (19). FTD was diagnosed according to the Lund–Manchester criteria (20). Patients underwent lumbar puncture for diagnostic purposes. CSF samples from 42 disease controls (FTD, schizophrenia, cognitively healthy probands; mean age: 56 ± 16.02 years; 16 male, 26 female) and 34 patients (mean age: 68 ± 7.74 years; 15 male, 19 female) with a clinical diagnosis of sporadic AD were analyzed to establish disease specific peptide patterns. The levels of Tau, pTau-181 and Aβ42 were measured for both AD and controls. Tau and pTau concentrations were higher and Aβ42 concentrations lower in the AD group compared with the controls, as expected. Values were 522 ± 337 vs 326 ± 287 pg/ml (mean ± SD) for Tau, 75 ± 35 vs 46 ± 18 pg/ml (mean ± SD) for pTau-181 and 327 ± 181 vs 502 ± 319 pg/ml (mean ± SD) for Aβ42, respectively.

Plasmids and Cloning

cDNA coding for human wild type APP (APPwt) or APP bearing the Swedish double mutation *K670N > M671L* (APPsw) was kindly provided by Dr. Bart De Strooper. The genes were excised from the pSG5 vector using *Sma*I and *Hind*III restriction enzymes and subcloned into the pcDNA3.1-/Neo vector using the *EcoRV* and *Hind*III restriction sites. Human Testican-1 cDNA was purchased from imaGenes (Berlin, Germany, GenBank: BC030691.2); it was excised from the shuttle vector (pBluescriptR) using *Sal*I and *Acc65*I restriction enzymes. The cDNA was subcloned into the pcDNA3.1-/Neo vector using the *Xho*I and *Acc65*I restriction sites. Selected clones were then sequenced and used for transient transfection. All reagents were from Thermo Fisher Scientific, Dreieich, Germany.

Cell Line Culture

Human Embryonic Kidney cells (HEK293) were purchased from Leibniz Institute DSMZ-German Collection of Microorganisms and Cell Cultures (ACC 305) and stably transfected with APPwt or APPsw. These were grown in DMEM (PAA, Cölbe, Germany) supplemented with 10% fetal bovine serum (PAA) and 1% G418 (Thermo Scientific Fisher) at 37 °C and 5% CO_2. For protein isolation 2×10^6 cells were plated in 6-well plates (Corning, Hamburg, Germany) and for immunocytochemistry 2×10^5 cells were plated on cover slips in 6-well plates 24 hours before beginning the experiment to reach confluence.

Transient Co-Transfection with Testican-1

Untransfected wild type, APPwt and APPsw HEK293T cells were grown in supplemented DMEM to confluence (90%–95%) and transfected with 8 μg of pcDNA3.1-/Neo empty vector (Mock) or pcDNA3.1-/Neo + Testican-1 using Lipofectamine 2000 (Thermo Fisher Scientific) for 24 hours, which was identified as the optimal transfection time. The expression of Testican-1 was analyzed by Western blot and immunocytochemistry. For immunocytochemistry, HEK293T cells were washed with phosphate-buffered saline (PBS) 3 times, fixed with 4% paraformaldehyde for 20 minutes and permeabilized with ice-cold acetone (−20 °C) for 5 minutes. Cells were then washed with PBS and incubated overnight with primary antibody (Testican-1, 6E10, GM130, Adaptin-γ, Rab4, and Rab9) (Supplementary Data Table S1) diluted in incubation buffer (PBS, 0.3% Triton X-100, 1% BSA) at 4 °C in a wet chamber. After washing with PBS, cells were incubated with FITC, Alexa Fluor 555 or Alexa Fluor 350 (Thermo Fisher Scientific) secondary antibody diluted in incubation buffer for 1 hour (Supplementary Data Table S2). Cells were further washed with PBS and mounted in slides using Fluoromount-G (Southern Biotech, Eching, Germany). Images were acquired with a confocal microscope (Leica TCS SP5, Wetzlar, Germany) and analyzed. Cells incubated only with secondary antibodies were used as negative control.

TABLE 1. Demographic and Neuropathological Data of Patients Included in the Western Blot Analysis

Group	Case	Source	Gender	AO	AoD	DD	Braak stage	CERAD score	ApoE Haplotype	PMI
Control	1	HUL								
Control	2	HUL								
Control	3	HUL								
Control	4	HUL								
Control	5	HUL								
% or Mean (SD)			F = 72.7%	69.1 (10.3)	77.3 (9.1)	10.8 (5.0)			ApoE4 = 22.5%	7.6 (4.7)
SAD	6	GNA	M	ND	67	ND	V	C	3/3	9.3
SAD	7	GNA	M	80	86	6	IV	C	ND	18.3
SAD	8	GNA	F	55	70	15	IV	B	3/4	11.8
SAD	9	GNA	F	79	87	8	V	C	3/4	2.8
SAD	10	GNA	F	82	>90	9	VI	C	3/3	4.5
SAD	11	GNA	F	58	79	21	II	C	ND	10.3
SAD	12	GNA	F	65	74	9	IV	C	3/3	2.5
SAD	13	GNA	F	65	76	11	V	C	4/4	4
SAD	14	GNA	F	69	76	7	VI	C	3/4	8
SAD	15	GNA	M	ND	83	ND	VI	C	3/2	4.5
SAD		GNA	F	ND	61	ND	VI	C	3/3	7.7
% or Mean (SD)			F = 72.7%	69.1 (10.3)	77.3 (9.1)	10.8 (5.0)			ApoE4=22.5%	7.6 (4.7)

AO, age of onset; AoD, Age of death; DD, disease duration; PMI, postmortem interval (hours); FC, frontal cortex; TC, temporal cortex; F, female; M, male; SAD, sporadic Alzheimer disease; SD, standard deviation; ND, not determined; GNA, Neuroscience Group of Antioquia; HUL, Hospital Universitari de Bellvitge.

Enzyme-Linked Immunosorbent Assay for Aβ40, Aβ42 Peptides, Tau, and pTau

The CSF levels of Aβ42, total Tau, and pTau-181 were measured using commercial enzyme-linked immunosorbent assay (ELISA) kits (Innogenetics, Ghent, Belgium), according to the manufacturer's protocol. The quantification of Aβ40 and Aβ42 levels in HEK293T cells transfected with Testican-1 was performed using ELISA kits and following the instructions of the manufacturer (Thermo Fisher Scientific). For this procedure 50 µL of primary antibody and 100 µL of conditioned medium were added to each well and incubated overnight at 4 °C. The plates were washed 4 times with washing buffer and incubated with secondary antibody coupled to peroxidase for 1 hour at room temperature and then further washed 4 times. Chromogen reagent was added and after 15 minutes. The reaction was stopped with stop solution. The absorbance was measured by using an ELISA reader at 450 nm. For each assay a standard curve was generated using synthetic Aβ40 and Aβ42 peptides and a well only with chromogen was used as blank.

Protein Isolation

Human frontal cortex and temporal cortex samples from 10 AD cases and 5 controls were cleared of meninges and only grey matter was used for the procedure; 250 mg of tissue was cut in small pieces, poured into a glass dounce tissue grinder type B and homogenized with 10 even strokes in 1 mL of lysis buffer containing 150 mM NaCl, 20 mM Tris pH 7.4, 1 mM EDTA, Glycerol 10%, 1% NP40, and a cocktail of phosphatase and protease inhibitors (Roche, Mannheim, Germany). The homogenate was centrifuged at 13.000 *g* for 10 minutes at 4 °C and the proteins present in the supernatant were quantified using the bicinchoninic acid method (BCA Protein Assay Kit, Thermo Fisher Scientific). The protein extracts were stored at −80 °C for further experiments.

HEK293T cells were washed with PBS and incubated for 20 minutes at 4 °C with lysis buffer (see above). Cell extracts were centrifuged at 13 000 *g* for 10 minutes and the proteins present in the supernatant were quantified by the BCA method. The protein extracts were stored at −80 °C for further experiments.

Sodium Dodecyl Sulfate Polyacrylamide Gel Electrophoresis

Once proteins were quantified, sodium dodecyl sulfate (SDS) polyacrylamide gel electrophoresis was carried out using a Miniprotean system (Bio-Rad, Munich, Germany). Samples were mixed with loading buffer (0.375 M Tris pH 6.8, 50% glycerol, 10% SDS, 0.5 M DTT, and 0.002% bromophenol blue) and heated to 95 °C for 5 minutes. Approximately 25–30 µg of protein were loaded into each well. After electrophoresis, proteins were transferred to nitrocellulose membranes using a Mini Trans-blot Electrophoretic Transfer Cell (Bio-Rad) at 300 mA for 2 hours. The membranes were incubated for 1 hour in 5% non-fat milk dissolved in TTBS (100 mM Tris pH 7.5, 500 mM NaCl, 0.02% Tween-20) and incubated overnight at 4 °C with primary antibody (Supplementary Data Table S1). Subsequently, membranes were washed with TTBS and incubated with secondary antibody (Supplementary Data Table S2) coupled to peroxidase for 1 hour at room temperature. Immunoreactive signal was developed with the ECL (enhanced chemiluminescence) Western Blotting chemiluminescence system (SuperSignal West Pico Chemiluminiscent Substrate, Thermo Fisher Scientific)

TABLE 2. Demographic and Neuropathological Data of Patients Included in the TMA Analysis

Group	Case	Source	Gender	AO	AoD	DD	Braak stage	CERAD score	ApoE Haplotype	PMI
Control	TMA_NP2	HH	F	ND	79	ND	0	0	ND	ND
Control	TMA_NP2	HH	M	ND	80	ND	3	0	ND	ND
Control	TMA_NP2	HH	F	ND	>90	ND	0	0	ND	ND
Control	TMA_NP2	HH	F	ND	>90	ND	0	0	ND	ND
Control	TMA_NP2	HH	M	ND	81	ND	0	0	ND	ND
Control	TMA_NP2	HH	F	ND	84	ND	0	0	ND	ND
Control	TMA_NP2	HH	M	ND	77	ND	0	0	ND	ND
Control	TMA_NP2	HH	F	ND	89	ND	0	0	ND	ND
Control	TMA_NP2	HH	F	ND	>90	ND	0	0	ND	ND
Control	TMA_NP2	HH	F	ND	80	ND	0	0	ND	ND
Control	TMA_NP2	HH	F	ND	54	ND	0	0	ND	ND
Control	TMA_NP2	HH	M	ND	44	ND	0	0	ND	ND
Control	TMA-NP3	HH	M	ND	71	ND	0	0	ND	ND
Control	TMA-NP3	HH	M	ND	67	ND	0	0	ND	ND
Control	TMA-NP3	HH	F	ND	86	ND	0	0	ND	ND
Control	TMA-NP3	HH	F	ND	82	ND	0	0	ND	ND
Control	TMA-NP3	HH	F	ND	84	ND	0	0	ND	ND
Control	TMA-NP3	HH	M	ND	84	ND	0	0	ND	ND
Control	TMA-NP3	HH	M	ND	69	ND	0	0	ND	ND
Control	TMA-NP3	HH	F	ND	82	ND	0	0	ND	ND
Control	TMA-NP3	HH	M	ND	58	ND	0	0	ND	ND
Control	TMA-NP3	HH	F	ND	72	ND	1	0	ND	ND
Control	TMA-NP3	HH	F	ND	88	ND	2	0	ND	ND
Control	TMA-NP3	HH	M	ND	65	ND	0	0	ND	ND
Control	TMA-NP3	HH	M	ND	56	ND	2	0	ND	ND
Control	ZTMA-44	HH	F	ND	81	ND	0	A	ND	ND
Control	ZTMA-44	HH	F	ND	75	ND	0	0	ND	ND
Control	ZTMA-44	HH	M	ND	>90	ND	0	0	ND	ND
Control	ZTMA-44	HH	M	ND	64	ND	0	0	ND	ND
Control	ZTMA-44	HH	M	ND	67	ND	0	0	ND	ND
Control	ZTMA-44	HH	M	ND	78	ND	0	0	ND	ND
Control	ZTMA-44	HH	M	ND	>90	ND	0	A	ND	ND
Control	ZTMA-44	HH	F	ND	81	ND	0	0	ND	ND
Control	ZTMA-44	HH	M	ND	86	ND	0	0	ND	ND
Control	ZTMA-44	HH	M	ND	61	ND	0	0	ND	ND
Control	ZTMA-44	HH	F	ND	66	ND	0	A	ND	ND
Control	ZTMA-44	HH	M	ND	>90	ND	0	0	ND	ND
	n	37								
	% female	48.6								
	mean	76.8								
	SD	12.4								
SAD	TMA_NP2	HH	F	ND	79	ND	5	B	ND	ND
SAD	TMA_NP2	HH	M	ND	80	ND	5	C	ND	ND
SAD	TMA_NP2	HH	F	ND	>90	ND	5	C	ND	ND
SAD	TMA_NP2	HH	F	ND	>90	ND	5	C	ND	ND
SAD	TMA_NP2	HH	M	ND	79	ND	3	B	ND	ND
SAD	TMA_NP2	HH	F	ND	86	ND	4	C	ND	ND
SAD	TMA_NP2	HH	M	ND	75	ND	3	C	ND	ND
SAD	TMA_NP2	HH	F	ND	89	ND	6	C	ND	ND
SAD	TMA_NP2	HH	F	ND	>90	ND	2	C	ND	ND
SAD	TMA_NP2	HH	F	ND	79	ND	6	C	ND	ND
SAD	TMA_NP2	HH	F	ND	54	ND	4	C	ND	ND
SAD	TMA_NP2	HH	M	ND	40	ND	5	C	ND	ND
SAD	TMA-NP3	HH	M	ND	72	ND	2	B	ND	ND

(continued)

TABLE 2 Continued

Group	Case	Source	Gender	AO	AoD	DD	Braak stage	CERAD score	ApoE Haplotype	PMI
SAD	TMA-NP3	HH	M	ND	86	ND	4	B	ND	ND
SAD	TMA-NP3	HH	F	ND	84	ND	5	B	ND	ND
SAD	TMA-NP3	HH	F	ND	80	ND	4	B	ND	ND
SAD	TMA-NP3	HH	F	ND	87	ND	4	C	ND	ND
SAD	TMA-NP3	HH	M	ND	68	ND	4	B	ND	ND
SAD	TMA-NP3	HH	M	ND	73	ND	2	C	ND	ND
SAD	TMA-NP3	HH	F	ND	81	ND	3	B	ND	ND
SAD	TMA-NP3	HH	F	ND	76	ND	4	B	ND	ND
SAD	TMA-NP3	HH	F	ND	>90	ND	5	C	ND	ND
SAD	TMA-NP3	HH	M	ND	66	ND	5	C	ND	ND
SAD	ZTMA-44	HH	F	ND	80	ND	5	C	ND	ND
SAD	ZTMA-44	HH	F	ND	89	ND	4	C	ND	ND
SAD	ZTMA-44	HH	M	ND	84	ND	4	C	ND	ND
SAD	ZTMA-44	HH	M	ND	69	ND	4	C	ND	ND
SAD	ZTMA-44	HH	M	ND	73	ND	3	C	ND	ND
SAD	ZTMA-44	HH	F	ND	82	ND	5	C	ND	ND
SAD	ZTMA-44	HH	F	ND	74	ND	6	C	ND	ND
SAD	ZTMA-44	HH	F	ND	79	ND	5	C	ND	ND
SAD	ZTMA-44	HH	M	ND	>90	ND	5	C	ND	ND
SAD	ZTMA-44	HH	F	ND	81	ND	5	C	ND	ND
SAD	ZTMA-44	HH	F	ND	>90	ND	3	C	ND	ND
SAD	ZTMA-44	HH	F	ND	>90	ND	6	C	ND	ND
	n	35								
	% female	62.9								
	mean	79.8								
	SD	11.5								

AO, age of onset; AoD, age of death; DD, disease duration; PMI, postmortem interval (hours); F, female; M, male; SAD, sporadic Alzheimer disease; SD, standard deviation; ND, not determined; HH, University Medical Center Hamburg-Eppendorf; TMA, tissue microarray.

and detected with a ChemiDoc system (Bio-Rad). The images were analyzed using the quantification software QuantityOne (Bio-Rad). The results of each sample were normalized to Actin or GAPDH and compared between groups. To minimize interassay variation, the samples from all experimental groups were processed in parallel.

Tricine Gel Electrophoresis

Protein extracts were loaded into each well with loading buffer (0.15 M Tris pH 6.8, 36% Glycerol, 12% SDS, 0.3 M DTT, 0.002% Coomassie blue) and heated to 95°C for 5 minutes before loading on precast 10%–20% Tricine gels. The gels were run using cathode buffer (1 M Tris base, 1 M Tricine (Thermo Fisher Scientific) and 1% SDS) anode buffer (1 M Tris base and 0.225 M HCl) and transferred to nitrocellulose membranes (Bio-Rad) using an electrophoretic transfer system (Bio-Rad) at 300 mA for 80 minutes. Membranes were blocked, incubated with primary and secondary antibodies (Supplementary Data Tables S1 and S2), and detected as described earlier.

TMA and Immunohistochemistry

Selected anatomically defined areas (frontal cortex, gyrus frontalis medius, temporal cortex at the level of the lateral corpus geniculatum and entorhinal cortex) from a total of 72 formalin-fixed (buffered neutral aqueous 4% solution), paraffin-embedded tissue specimens (35 AD patients and 37 controls) were used for TMA generation.

A total of 8 tissue cylinders (0.6 mm of diameter) were punched from anatomically defined areas of a donor tissue block using a semiautomatic robotic precision instrument and brought into 3 different recipient paraffin blocks, each containing 356 individual samples. Multiple 4-μm sections of the resulting TMA block were cut, mounted to an adhesive-coated slide system and further processed for histological staining according to standard protocols (21). Immunohistochemistry was performed using appropriate antigen retrieval methods with internal controls. For the detection of neuritic plaques, the primary antibody 6E10 (Covance, Munster, Germany) directed against Aβ was used. An affinity-purified polyclonal antibody against Testican-1 was used at a dilution of 1:100. Primary antibodies were visualized using a standard diaminobenzidine streptavidin-biotin horseradish peroxidase method (Sigma-Aldrich, Munich, Germany). Quantification of diffuse plaques, neuritic plaques, and Testican-1-positive deposits was accomplished by counting positive signals for Aβ and Testican-1 on consecutive sections. The average of positive signals was determined for each region of patients/controls by calculating the mean value of all assessed tissue specimens. In

average, 6.9 out of 8 tissue specimens in 1 row could be analyzed. A region was considered analyzable if at least 2 tissue specimens could be assessed. A total of 5 regions had to be excluded from analysis due to poor quality.

CSF Capillary Electrophoresis–Mass Spectrometry Analysis

Cerebrospinal fluid sample collection and its analysis was performed as described previously in (9). Briefly, CSF was centrifuged immediately after collection (1600 g, 4 °C, 15 minutes), aliquoted into polypropylene test tubes (each aliquot, 750 µL), frozen within 30–40 minutes after the puncture and stored at −80 C until use. After thawing, 700 µL of CSF were diluted with 700 µL buffer (pH 10.5; 2 M urea, 100 mmol/L NaCl, 0.0125% NH_3) and ultracentrifuged using Centrisart ultrafiltration devices (cut off 20 kDa) at 4 °C until 1.1 mL of filtrate was obtained. Subsequently the filtrate was applied onto a PD-10 desalting column (Amersham Biosciences, Freiburg, Germany) equilibrated in 0.01% NH_4OH in HPLC-grade water (Roth, Karlsruhe, Germany), and the eluate was lyophilized, stored at 4 °C and resuspended in 10 µL HPLC-grade water before capillary electrophoresis–mass spectrometry (CE-MS) analysis. CE-MS analysis was performed as described using a P/ACE MDQ (Beckman Coulter, Krefeld, Germany) system on-line coupled to a Micro-TOF MS (Bruker Daltonic, Bremen, Germany) (9, 22–24).

Statistical Analysis

Statistical analysis was carried out in GraphPad Prism 4 (La Jolla, CA, USA) and SPSS 17 for Windows (Chicago, IL, USA). The Fisher exact test for homogeneity of variances was used to determine the appropriateness of parametric or nonparametric analysis. The data from the histological analysis and the cell cultures were evaluated using a 2-tailed *t*-test setting alpha value at $p < 0.05$. Western blot and ELISA (Aβ42, total Tau, and pTau-181) data from human brain samples were analyzed using Mann-Whitney U-test to determine significant differences between 2 independent groups. Alpha value was set to $p < 0.05$. For the cell culture at least 4 independent experiments were conducted for each study in the protein level characterization. The data analyzed were expressed as mean ± SEM.

The list of Testican-1 peptides was obtained by the comparison of all available data sets (e.g. control vs. AD, FTD and schizophrenia patients) with MosaCluster software package (25) and the results were validated. Subsequently, the preliminary biomarker patterns were refined by employing an unadjusted p value limit of 0.01 and using one-out cross-validation to attain high sensitivity and specificity. Estimates of sensitivity and specificity were calculated based on tabulating the number of correctly classified samples. The receiver operating characteristic (ROC) curve was obtained by plotting all sensitivity values (true positive fraction) on the y-axis against their equivalent (1-specificity) values (false positive fraction) for all available thresholds on the x-axis (MedCalc Software, Mariakerke, Belgium, www.medcalc.be). The area under the ROC curve (AUC) was evaluated as it provides a single measure of overall accuracy that is not dependent upon a particular threshold.

RESULTS

Testican-1 Accumulates and Co-Aggregates with Amyloid Plaques in Brain Tissue of AD Patients

Based on our previous findings with human samples (9), we evaluated the levels of Testican-1 in brain homogenates from AD patients and cognitively healthy individuals. The results showed steady-state levels of Testican-1 in the frontal and temporal cortex of AD patients compared with controls (frontal cortex: $p = 0.0280$; temporal cortex: $p = 0.0027$) (Fig. 1A, B).

Immunohistochemical analysis revealed that Testican-1 was present in cortical neurons of healthy brain tissue (Fig. 1C), while Testican-1 deposits were identified in AD presenting with granulovacuolar degeneration (Fig. 1D), ghost tangles (Fig. 1E), and exhibiting an extracellular plaque-like accumulation pattern in the cerebral cortex of AD patients (Fig. 1K; Table 3) following dense or diffuse distribution (Fig. 1F–H, K; Supplementary Data Fig. S1A). In fact, Testican-1 deposits colocalized with amyloid plaques (Fig. 1I). The average number of diffuse (poorly marginated) and neuritic (dense-core) plaques and the total number of plaques per tissue punch was determined for AD patients and controls, as previously described in (21); this analysis showed significantly higher plaque loads in AD patients compared with controls (Fig. 1J; Table 3). Accordingly, the number of Testican-1-positive deposits was assessed. We found a distribution pattern of Testican-1 plaques similar to that of total Aβ plaques, with increased Testican-1-positive deposits count in the frontal and temporal region and a decreased load in the entorhinal cortex (Fig. 1J; Table 3). The mean ratio of Aβ-positive to Testican-1-positive deposits was 20.4:1 in the frontal cortex, 5.6:1 in the temporal cortex and 8.7:1 in the entorhinal cortex, revealing that the highest relative and absolute number of Testican-1-positive deposits were in the temporal cortex. There was a significant positive correlation of the number of Testican-1-positive deposits to the amount of neuritic or dense plaques both in the frontal and temporal cortex ($r = 0.66$, $p < 0.001$ and $r = 0.36$, $p < 0.05$, Supplementary Data Fig. S1B), but not in the entorhinal cortex ($r = 0.12$, $p = 0.33$) (data not shown). No correlations were seen between the number of total Aβ plaques or the number of diffuse Aβ plaques and Testican-1 accumulation in any of the assessed brain regions (data not shown). Furthermore, Testican-1 deposits did not correlate with phosphorylated Tau deposits or microglial immunoreactivity in the AD brains studied (Fig. 1K). These findings suggest that Testican-1 accumulation and aggregation with Aβ plaques may be caused by impairment of the clearance mechanisms in the brain of AD patients, as reported by other studies (6, 26).

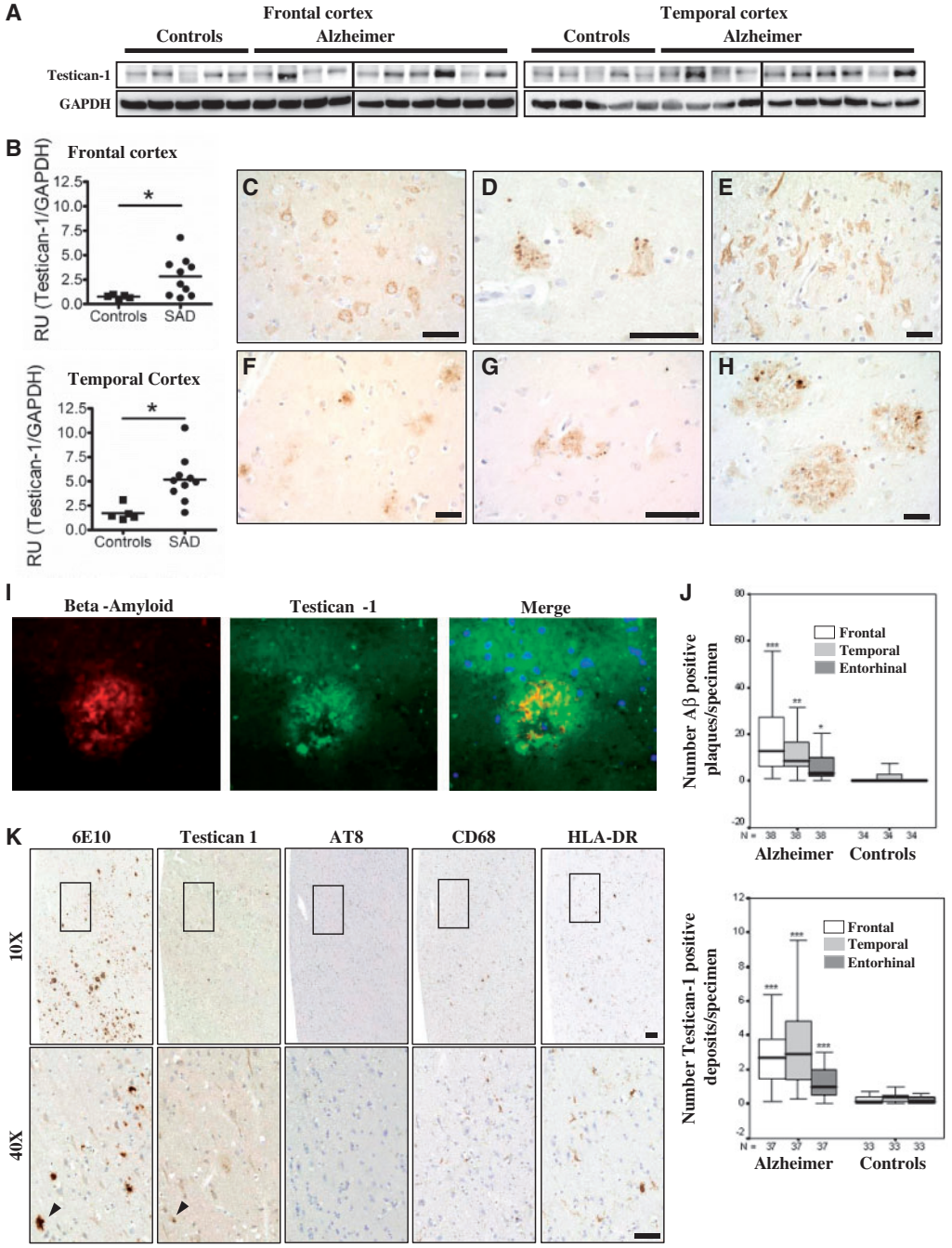

FIGURE 1. Protein levels and histological characterization of Testican-1 in human brain tissue. **(A)** Western blots of Testican-1 in frontal cortex and temporal cortex homogenates from healthy individuals and sporadic AD patients. **(B)** Dot-plot graphs of Testican-1 in frontal cortex and temporal cortex homogenates from healthy individuals and sporadic AD patients (FC: $p = 0.0280$, TC: $p = 0.0027$, RU = Relative units). Testican-1 immunostaining showing Testican-1 immunoreactivity in cortical neurons in a control case **(C)**, neurons with granulovacuolar degeneration in an AD case **(D)**, ghost tangles **(E)**, and small cell processes within diffuse amyloid plaques **(F–H)**. **(I)** Immunofluorescence staining of an Aβ plaque showing colocalization of Aβ and Testican-1. **(J)** Number of Testican-1- and Aβ-positive deposits per specimen in TMAs of AD patients and controls using immunohistochemical staining. Results are means of an average of 6.9 tissue samples per region per patient. The black lines within the boxes represent medians; the boxes encompass 25th and 75th percentiles of the distribution; the whisker indicates the range of values. Results were analyzed using a Student *t*-test; ***$p < 0.001$, **$p < 0.005$, *$p < 0.05$. **(K)** Immunohistochemical staining of frontal cortex sequential sections of an AD case for amyloid beta (6E10), Testican-1, hyperphosphorylated Tau (AT8), and microglial markers (CD68 and HLA-DR). Only some Testican-1 deposits showed spatial correlation with amyloid plaques (black arrowheads). Testican-1 deposits were not associated with Tau deposits or microglial staining. Scale bars = 50 μm.

TABLE 3. TMA Plaque Counts for Testican-1 and β-Amyloid

	Testican-1					β-Amyloid														
						Total Plaques					Neuritic Plaques					Diffuse Plaques				
	AD		Controls			AD		Controls			AD		Controls			AD		Controls		
Brain region	Mean	SD	mean	SD	p	mean	SD	mean	SD	p	mean	SD	mean	SD	p	mean	SD	mean	SD	p
Frontal cortex	3.3[a]	3.0	0.3[b]	0.5	<0.001	18.7	16.8	0.7	2.4	<0.001	0.6	0.7	0.0	0.1	<0.001	18.1	16.4	0.7	2.4	<0.001
Temporal cortex	3.6[a]	2.7	0.4	0.4	<0.001	12.0	9.8	3.5	11.9	<0.005	0.5	0.5	0.1	0.1	<0.001	11.5	9.6	3.5	11.8	<0.005
Entorhinal cortex	1.4	1.2	0.3	0.4	<0.001	6.6	7.2	2.3	7.5	<0.05	0.1	0.2	0.1	0.3	0.29	6.5	7.1	2.2	7.2	<0.05

SD, standard deviation; AD, Alzheimer disease (n = 35); Controls (n = 37), except: [a]n = 37, [b]n = 33. Between group differences were calculated using Student *t*-test.

Increased Levels of Testican-1 CTFs in the CSF of AD Patients

The accumulation of Testican-1 in the same brain regions characterized by Aβ aggregation and plaque formation suggest that both proteins may coexist in extracellular compartments during the neurodegenerative process. Here we report the identification of 10 Testican-1 fragments in CSF from AD patients (Table 4), which displayed higher detection frequencies and mean amplitude (Supplementary Data Fig. S1C; Table 4). The overall AUC for fragments in the training set was calculated as 0.973 (95% CI: 0.908–0.996; SEM: 0.020; p-value = 0.0001). For comparison using cut-off values of >61 pg/mL for pTau-181 and <500 pg/mL for Aβ42, sensitivity for AD was 80% for pTau-181 and 81% for Aβ42; specificity was 85% for pTau-181 and 42% for Aβ42 in our sample. These results confirm our previous finding of the presence of Testican-1 in CSF samples from AD patients (9), and suggest that this proteoglycan could be used as an indicator of the pathologic state.

Subcellular Distribution of APP and Testican-1 in HEK293T Cells

To identify a possible role for Testican-1 in APP processing or Aβ aggregation, we used stable HEK293T cells expressing the human wild type form of APP (APPwt) or the APP variant bearing the Swedish double mutation *K670N > M671L* (APPsw) to establish whether APP and Testican-1 displayed the same subcellular distribution. Wild type HEK293T cells were used as negative control because of their sparse expression of APP. In these cells, Testican-1 was found close to the nucleus in a region that corresponds to the endoplasmic reticulum, whereas APP was distributed along the cytoplasm and showed intense perinuclear labeling (Fig. 2). The expression of APP and Testican-1 in APPwt cells displayed a puncta-like pattern with few colocalization areas in cytoplasm (Fig. 2). In contrast, the colocalization analysis of APP and Testican-1 in APPsw cells demonstrated that both proteins have a diffuse distribution pattern and colocalize in the same regions of the cytoplasm (Fig. 2).

Previous studies demonstrated that the intracellular traffic and processing of APPwt differs from that of APPsw (27, 28). We analyzed the distribution of APP and Testican-1 in the endocytic pathway using the early endosomal marker Rab4. The images show that only the HEK293T cells bearing the Swedish mutation transfected with Testican-1 presented colabeling points for APP and Rab4 (Fig. 3A). In contrast, both APPwt and APPsw cells transfected with Testican-1 showed Rab4-positive puncta labeled with Testican-1 (Fig. 3A), although the costaining was more intense in APPwt cells. In additional experiments the localization of APP and Testican-1 in late endosomes was evaluated using Rab9 as a marker. The results showed no changes in the distribution and staining pattern of both proteins in transfected cells (Fig. 3B). The presence of the mutant APP and Testican-1 in early endosomes suggests that the mutant protein may modify the traffic of the proteoglycan affecting the distribution in the endosomal compartment. Thus, we used the trans-Golgi network (TGN) marker Adaptin-γ to determine if Testican-1 was translocated to the TGN. Surprisingly, we observed that Testican-1 had the same subcellular distribution as the TGN marker in all cell lines with some aggregates present in wild type cells and a clear distribution around the nucleus in APPwt and APPsw cells (Fig. 4A). In further experiments using the marker GM130 to label the Golgi apparatus, Testican-1 colocalized with GM130 in APPwt and APPsw cells showing a punctate pattern. In APPwt cells, the costaining was restricted to the perinuclear region corresponding to the Golgi apparatus, whereas in APPsw cells, the colabeling was present not only in this region but in the rest of the cytoplasm. This observation may be interpreted as transport vesicles carrying Testican-1 (Fig. 4B).

Co-Expression of Testican-1 and Mutant APP Decreased the Production of Aβ Peptides HEK293T Cells

To explore whether the observed differential sorting of Testican-1 caused by APP expression was related to its processing, HEK293T cells (WT, APPwt, and APPsw) were transiently transfected either with Testican-1 or empty vector for 24 hours; after that time, the supernatant was collected and used to measure the production of Aβ40 and Aβ42 with an ELISA test. The analysis showed reduced levels of both Aβ40 (Mean Concentration = 623.1 pg/mL; SEM = 6.507;

TABLE 4. Testican-1 Peptides Present in CSF from AD Patients and Controls

Protein ID	Mass (Da)	Sequence of Testican Fragments	Amino Acid No.	CE time (minutes)	AD			Control			P value (unadjusted)	AUC
					F	MA	SD	F	MA	SD		
49413	1552.61	VTEDDEDEDDDKE	420–432	30.78	26	109.71	113.95	25	61.65	66.66	0.03	0.69
53580	1623.65	AVTEDDEDEDDDKE	419–432	31.10	23	401.39	452.59	25	171.11	220.61	0.16	0.62
59244	1738.68	AVTEDDEDEDDDKED	419–433	32.16	22	45.88	57.53	14	16.40	27.78	0.02	0.70
61093	1796.68	VTEDDEDEDDDKEDE	420–434	32.60	15	29.93	51.25	9	10.51	27.91	0.08	0.63
64448	1867.72	AVTEDDEDEDDDKEDE	419–434	33.07	24	832.84	879.61	28	707.23	799.14	0.20	0.61
67398	1915.72	EDDEDEDDDKEDEVGY	422–437	34.24	29	138.15	106.15	28	92.21	91.08	0.09	0.65
71134	2023.81	AVTEDDEDEDDDKEDEVG	419–436	33.58	26	622.70	561.23	33	505.32	427.04	0.21	0.61
77995	2186.87	AVTEDDEDEDDDKEDEVGY	419–437	34.39	6	369.53	1198.71	10	915.31	2034.48	0.22	0.56
82190	2299.94	AVTEDDEDEDDDKEDEVGYI	419–438	34.61	16	110.18	296.69	18	42.94	67.39	0.79	0.52
89021	2486.04	AVTEDDEDEDDDKEDEVGYIW	419–439	35.76	24	1469.97	1450.83	30	1444.68	1385.66	0.49	0.56

Protein ID; molecular mass (in Dalton). Amino acid positions in the protein (SwissProt accession number: Q08629). Elution times in CE. The observed frequency (F) of occurrence and the corresponding MAs in AD and control patients. Unadjusted p-values and AUC. SD, Standard deviation. p = 0.0001.

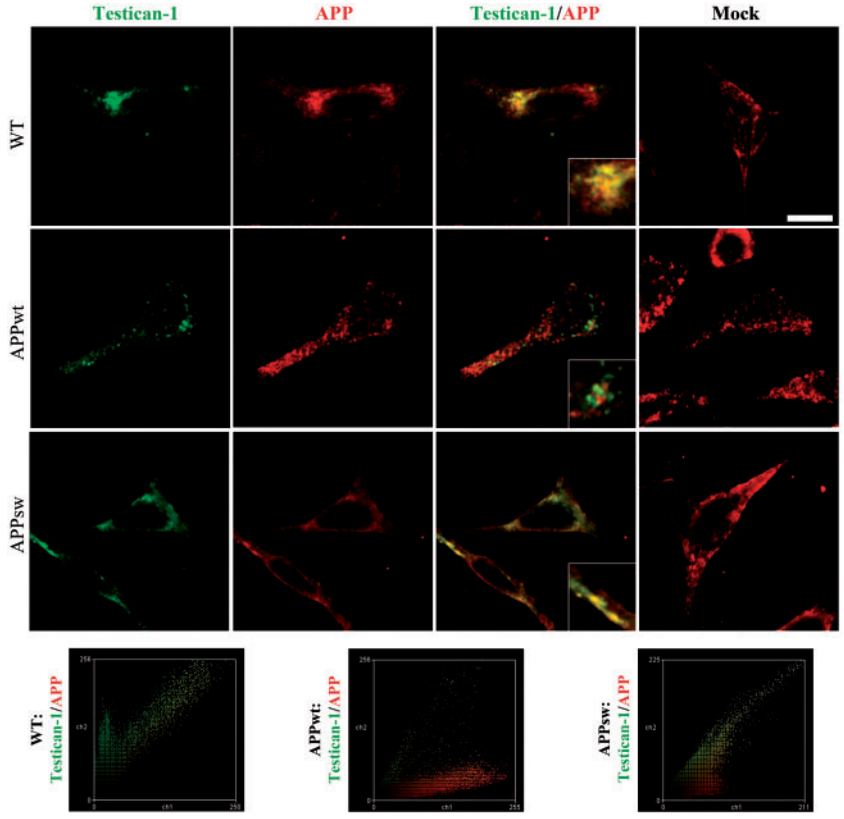

FIGURE 2. Subcellular distribution of Testican-1 and APP in HEK293T cells. Untransfected HEK cells and cells expressing APPwt and APPsw were cotransfected with Mock or Testican-1. The distribution of APP (red) and Testican-1 (green) was analyzed 24 hours after transfection using confocal microscopy. Colocalization plots are shown at the bottom. Scale bar = 10 μm.

p = 0.0207) and Aβ42 (Mean Concentration = 38.25 pg/mL; SEM = 3.512; p = 0.0011) in APPsw cells transfected with Testican-1 vs the control (Aβ40 Mean Concentration = 769.9 pg/mL; SEM = 4.547; Aβ42 Mean Concentration = 56.55 pg/mL; SEM = 1.074) (Fig. 5A). In contrast, the levels of Aβ40 and Aβ42 in APPwt or wild type were not altered by Testican-1 transfection (Fig. 5A).

It is possible that decreased levels of Aβ40 and Aβ42 in APPsw cells transfected with Testican-1 were related to Testican-1 influence at different points during either the production or the degradation of Aβ. To examine whether Testican-1 could regulate Aβ production, we analyzed the levels of full-length APP using Western blot. The analysis demonstrated that the presence of Testican-1 produces a

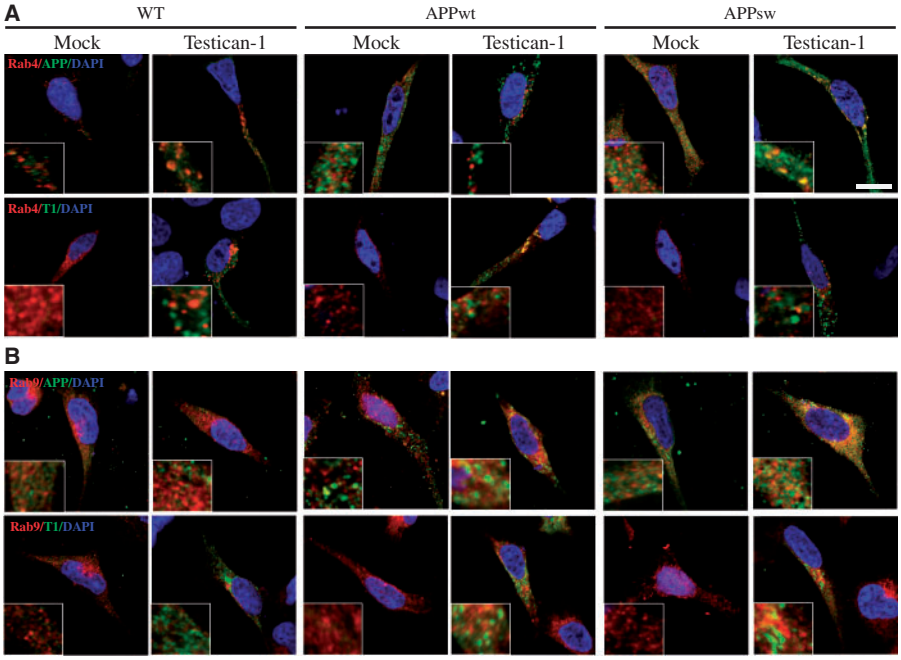

FIGURE 3. Subcellular localization of Testican-1 and APP in the endocytic pathway of HEK293T cells. Untransfected HEK cells and cells expressing APPwt and APPsw were cotransfected with Mock or Testican-1. **(A)** Representative pictures of a double staining showing the localization of Testican-1 or APP (green) and Rab4 (red). Testican-1 and APP colocalize with Rab4 in APPsw cells showing a puncta pattern. **(B)** APP and Testican-1 (green) localization with the late endosome marker Rab9 (red) was analyzed 24 hours after transfection using confocal microscopy. Neither the shape, distribution nor colocalization of Rab9 is modified in APPwt and APPsw cell lines after Testican-1 transfection. Scale bars = 10 μm.

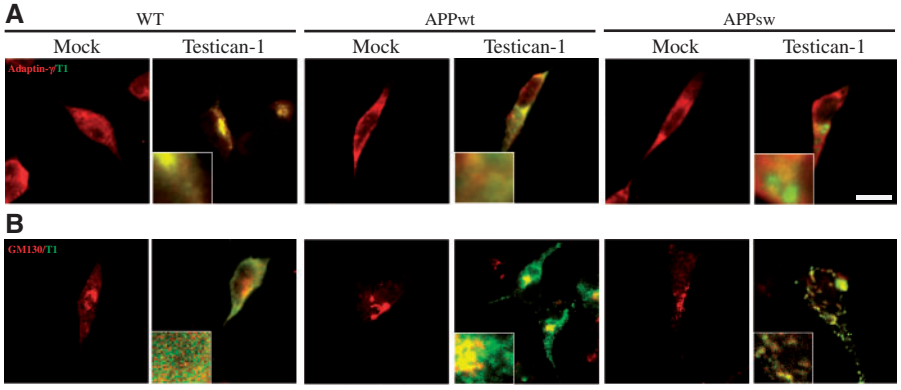

FIGURE 4. Sorting of Testican-1 into the TGN of HEK293T cells. Untransfected HEK cells or cells expressing APPwt and APPsw were cotransfected with Mock or Testican-1 and analyzed 24 hours after transfection using confocal microscopy. **(A)** Testican-1 (green) localization in the TGN labeled by Adaptin-γ (Red) was evaluated 24 hours after transfection. Testican-1 colocalizes with Adaptin-γ in all the cell lines analyzed. **(B)** Testican-1 (Green) localization with the Golgi marker GM130 (Red) was analyzed 24 hours after transfection. Testican-1 was located in the Golgi apparatus and transport vesicles of the APPsw cells. Scale bar = 10 μm.

significant accumulation of APP in APPsw cells ($p = 0.05$) (Fig. 5B). This effect was also observed in APPwt cells transfected with Testican-1 but the differences failed to reach statistical significance (Fig. 5B). To examine whether Testican-1 could regulate Aβ production, we analyzed the relative activity of the enzymes involved in the processing of APP by monitoring levels of APP CTFs, C83 and C99 using Western blot. The first fragment serves as an indirect measure of the α-secretase activity and the second reflects the activity of the β-secretases. The analysis demonstrated that the presence of Testican-1 did not alter α- or β-secretase activity (Supplementary Data Fig. S2A). To confirm these results we also evaluated the levels of APP, APP CTFs, and presenilin-1 (PS1) in brain samples from control and SAD individuals. However, no significant changes were observed in any of the proteins evaluated in frontal and temporal

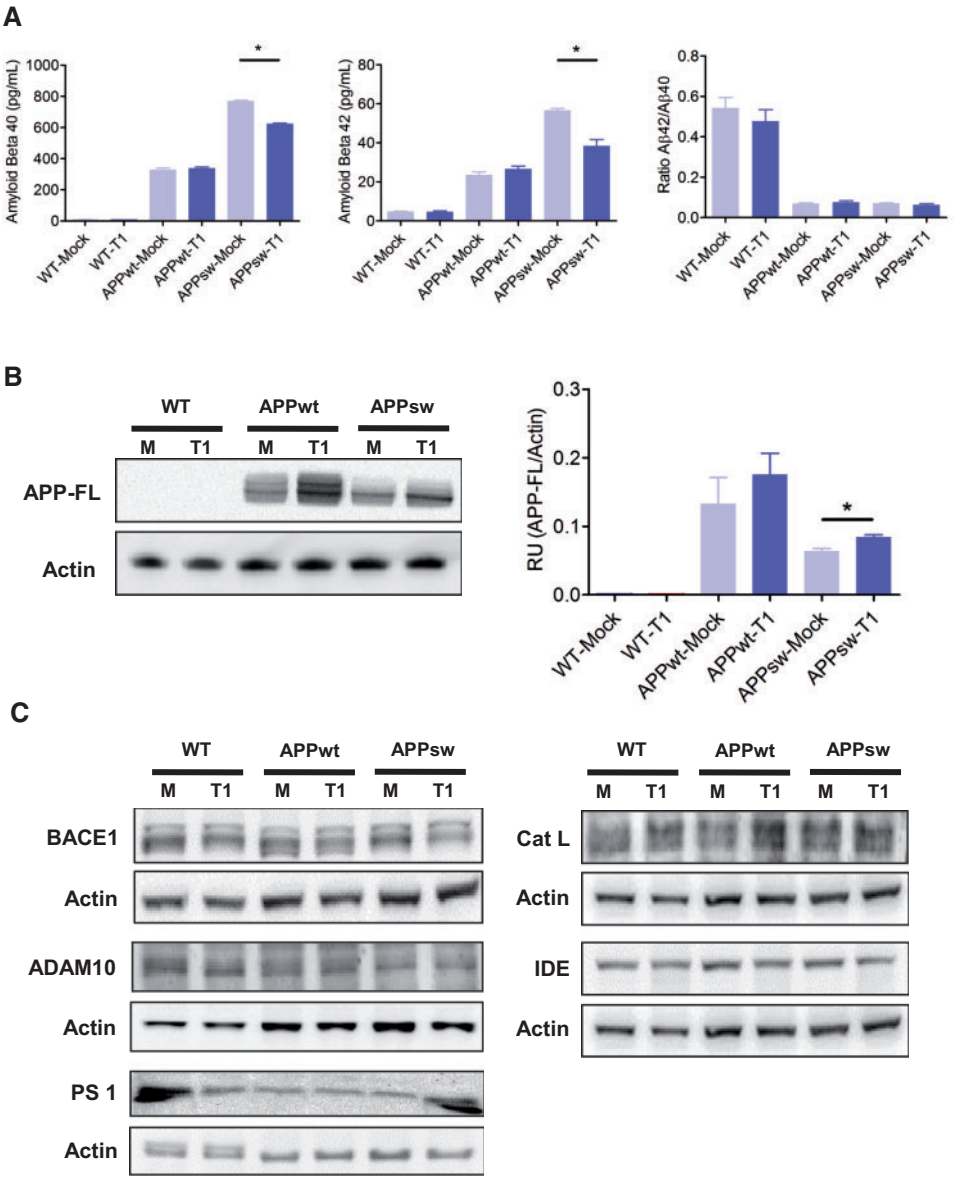

FIGURE 5. Protein levels of Aβ, APP, and enzymes involved in the processing of APP and degradation of Aβ in HEK293T cells. **(A)** Levels of Aβ40, Aβ42, and Aβ42/Aβ40 ratio in supernatant from HEK293T cells transfected with Testican-1. After 24 hours, the levels of Aβ40 and Aβ42 present in the supernatant were measured by ELISA. A significant decrease in the concentration of Aβ40 ($p < 0.0001$) and Aβ42 ($p = 0.0006$) was observed in the HEK cells expressing APPsw. Results were analyzed using a *t*-test; $p < 0.05$ was considered significant. Data are expressed as mean ± SEM. **(B)** Representative Western blots and histograms APP full-length from HEK293T cells (WT, APPwt, and APPsw) transfected with empty vector (Mock) or Testican-1. Decreased levels of APP were visible for APPsw cells ($p = 0.05$, RU = Relative units). **(C)** Representative Western blots of BACE1, ADAM10, PS1, cathepsin-L, and IDE in HEK293T cells (WT, APPwt, and APPsw) transfected with empty vector (Mock) or Testican-1.

cortices from control and SAD samples (Supplementary Data Fig. S2B, C).

Because APP levels seemed to be altered by Testican-1, we analyzed whether this proteoglycan could also modify the expression of APP processing enzymes BACE1, ADAM10, and PS1 in cell lysates. However, no significant changes were observed in any of these proteins (Fig. 5C). Finally, we considered the possibility that Testican-1 may alter degradation of Aβ; thus, we determined levels of cathepsin-L and insulin degrading enzyme (IDE). The first is a protease shown to be involved in Aβ degradation (29) and inhibited by Testican-1 (30), and the second is a neutral thiol metalloprotease (31) capable to degrade small peptides including insulin, insulin-like growth factors I, II, and Aβ (32–34). Despite some variation on the expression levels of these proteins, we could not find differences among the experimental groups (Fig. 5C). These results indicate that Testican-1 reduces the levels of Aβ40 and Aβ42, yet does not affect the expression of enzymes

required for processing or degradation of Aβ in HEK cells. Instead, it seems to prevent the processing or clearance of APP by altering the activity of these enzymes.

DISCUSSION

To date, Testican-1 has been identified as an extracellular matrix proteoglycan, enriched in brain and as a cysteine protease inhibitor (35). The presence of Testican-1 fragments in the CSF of AD patients (9) was intriguing because of the seemingly unrelated biological function of Testican-1 and AD pathophysiology. This prompted us to perform further experiments and explore the role of Testican-1 in AD.

Western blot analysis detected significant differences in Testican-1 levels in the frontal cortex of sporadic AD patients compared with controls using Western blot, suggesting that increased amounts of Testican-1 are relevant for its deposition in plaques. Given that proteoglycans play an important role in establishing and maturation of synapses, this may indicate loss of synaptic function caused by neuronal death (36). Furthermore, in view of Testican-1 expression in astrocytes after some types of injuries, it is possible that neurons are not the only source of Testican-1 in AD brains (15).

The morphological analysis showed the presence of Testican-1 in Aβ plaques of brain tissue from AD patients. Similar to the results of Aβ plaque counts, accumulation of Testican-1 was seen to a much lesser extent, in non-demented controls than in AD patients. It is known that Aβ binds to several biomolecules including proteoglycans, which can promote the aggregation of Aβ species and form amyloid fibrils (37, 38). Although Aβ self-aggregates, the interaction with proteoglycans and heparan sulfate proteoglycans contributes to the amyloid accumulation and fibril formation process (39, 40). It has been shown that different proteoglycans including several syndecans, agrin and glypican-1 are associated with amyloid plaques (41, 42). Our study reveals that Testican-1 plaques had an accumulation pattern that parallels amyloid-plaque distribution (frontal = temporal > entorhinal); moreover, Testican-1 plaque load was positively correlated with neuritic plaque load in the frontal and temporal cortex, but not with diffuse Aβ plaque load. Neuritic plaques are thought to be formed from diffuse plaques and represent a later stage of plaque maturation during AD pathophysiology (2). The presence of Testican-1 defines a new subtype of AD plaque, the pathophysiological implications of which are unclear. Nonetheless, proteoglycans are the main component of the brain extracellular matrix, which is tightly involved in the regulation of the structure of pre- and postsynaptic terminals during neuronal activity (43). Therefore, co-aggregation of Testican-1 and other proteoglycans with amyloid plaques may indicate an underlying neurodegenerative process.

The presence of Testican-1 CTFs in the CSF of AD patients suggests that Testican-1 might be undergoing a processing in AD that could be related to that of APP. The CTF region of Testican-1 contains a cluster of glutamic acid and aspartic acid residues, which compose 40% of the C-terminal residues. Similar domains of 9 acidic amino acids are also found in other proteins, e.g. APP (44), claustrin (45), versican (46), and brevican (47). This acidic sequence may be involved in the interaction with cationic compounds. Testican-1 is mainly found in postsynaptic densities of CA3 hippocampal neurons (48), where it is likely to associate with components of the postsynaptic membrane, modulating the binding of ligands to target cells, and influencing the development and function of synapses (as observed with glypican, a proteoglycan with a structure similar to that of Testican-1 [49]). The loss of synapses and the neuronal death are driving events leading to the cognitive decline observed in dementia. Changes in synaptic proteins could point toward early stages of neurodegeneration.

The characterization studies performed during the enrollment of volunteers suggest that the ratio Testican-1 CTFs/Aβ42 and Testican-1 CTFs/Tau/pTau could be used as a confirmatory diagnostic tool in AD patients. Thus, synaptic peptides such as Testican-1 in CSF may be suitable markers for diagnosing AD or for defining a subgroup of AD patients. Nonetheless, because of the limited number of individuals in our study, these questions need to be investigated in a greater prospective sample.

The analysis of the subcellular distribution of Testican-1 and APP in HEK293T cells showed that both proteins seemed to be localized in the same subcellular compartment. However, some differences were observed between the distribution pattern of APPwt and APPsw independently of the transfection with Testican-1. The former showed a puncta-like pattern characteristic of vesicular structures while the latter displayed a diffuse pattern. Furthermore, we evaluated the effect of APP in the sorting of Testican-1 into the endocytic pathway. It is known that in non-neuronal cells, APP remains for short time at the cell surface. After endocytosis, part of the APP is recycled to the plasma membrane and the rest is delivered to endosomes (50, 51). Previous reports demonstrated that endocytosis of APP is critical for the production of Aβ because endosomes are the major site where BACE1 cleaves APP (27, 52). However, there are differences in the subcellular localization with respect to processing of APP variants. For example, it has been shown that APPwt is reinternalized and recycled before processing by BACE1 during the transit through the endocytic pathway (27, 53), whereas the mutant form APPsw is cleaved by BACE1 during early stages of the nascent protein in the Golgi apparatus, which is part of the secretory pathway (28, 53). Our data show that in APPwt cells, APP and Testican-1 are transported from the TGN to early endosomes and then secreted out of the cells. On the other hand, in APPsw cells Testican-1 and APPsw are enriched in Rab4-positive early endosomes while no labeling was observed in late endosomes indicating that both proteins were translocated from the TGN to early endosomes where both proteins seemed to colocalize. This could induce the mutant APP and Testican-1 to be transported again to the TGN to further secretion out of the cell. The translocation of both proteins to the TGN could lead to the accumulation and sequestration of APPsw and Testican-1 into the Golgi network. This possibility is supported by our observation that Testican-1 was in the same subcellular location as the TGN marker Adaptin-γ. In addition, the distribution of Testican-1 in GM130-positive vesicles observed in APPsw cells is in concordance with previous work describing the early processing of APPsw in secretory vesicles (28, 53). The accumulation of Testican-1 and APPsw

in the TGN may override the processing capability of the β-secretases leading to decreased levels of Aβ species.

Our in vitro experiments, our *in vitro* experiments demonstrated that transient transfection of HEK293T cells stably expressing wild type or mutant APP with Testican-1 decreased the levels of Aβ40 and Aβ42 in APPsw cells. Also, we showed that the expression of full-length APP was elevated in APPsw cells probably caused by its accumulation in the TGN and not by altered protein levels or activity of α-, β-, or γ-secretases, as demonstrated by the analysis of APP CTFs and the production of Aβ species. We also found that the expression of degrading enzymes such as cathepsin-L and IDE appeared unchanged. Our experiments indicate that the coexpression of APPsw and Testican-1 might influence APPsw sorting thereby decreasing Aβ generation. Nevertheless, the findings do not exclude the possibility that Testican-1 might reduce Aβ production by inhibiting the proteolytic action of BACE1 or other secretases.

Although the modulation of Aβ levels by Testican-1 is specific of mutant APPsw, the interaction of Testican-1 with the wild type form of APP may be relevant to understand the dynamic of the protein and the aggregation process as demonstrated by the experiments performed in human samples.

In conclusion, Testican-1 seems to be involved in the pathophysiology of AD as seen both in human brains and *in vitro*. This involvement may be related to a new function of Testican-1 in APP sorting through the endocytic pathway. Our findings on the role of Testican-1 in Aβ production and APP sorting, however, do not explain the presence of Testican-1 in neuritic plaques or the specific increase of its fragments in AD patients. Further studies are required to determine the detailed molecular mechanisms and their relevance *in vivo*.

ACKNOWLEDGEMENTS

Authors would like to thank Dr. Bart De Strooper for the APP cDNAs, the Light Microscope Facility at Campus Forschung-UKE for confocal imaging assistance and to Dr. Francisco Lopera and Dr. Andres Villegas from the Brain bank of the University of Antioquia for supplying AD brain tissue for human assays.

REFERENCES

1. Querfurth HW, LaFerla FM. Alzheimer's disease. N Engl J Med 2010; 362:329–44
2. Yamaguchi H, Nakazato Y, Hirai S, et al. Electron micrograph of diffuse plaques. Initial stage of senile plaque formation in the Alzheimer brain. Am J Pathol 1989;135:593–7
3. Buckner RL, Snyder AZ, Shannon BJ, et al. Molecular, structural, and functional characterization of Alzheimer's disease: evidence for a relationship between default activity, amyloid, and memory. J Neurosci 2005;25:7709–17
4. Thal DR, Rüb U, Orantes M, et al. Phases of A -deposition in the human brain and its relevance for the development of AD. Neurology 2002;58: 1791–800
5. Scheuner D, Eckman C, Jensen M, et al. Secreted amyloid -protein similar to that in the senile plaques of Alzheimer's disease is increased in vivo by the presenilin 1 and 2 and APP mutations linked to familial Alzheimer's disease. Nat Med 1996;2:864–70
6. Mawuenyega KG, Sigurdson W, Ovod V, et al. Decreased clearance of CNS - -amyloid in Alzheimer's disease. Science 2010;330:1774
7. Liao L, Cheng D, Wang J, et al. Proteomic characterization of postmortem amyloid plaques isolated by laser capture microdissection. J Biol Chem 2004;279:37061–8
8. Armstrong A, Mattsson N, Appelqvist H, et al. Lysosomal network proteins as potential novel CSF biomarkers for Alzheimer's disease. Neuromolecular Med 2014;16:150–60
9. Jahn H, Wittke S, Zürbig P, et al. Peptide fingerprinting of Alzheimer's disease in cerebrospinal fluid: identification and prospective evaluation of new synaptic biomarkers. PLoS One 2011;6:e26540
10. Bonnet F, Perin JP, Maillet P, et al. Characterization of a human seminal plasma glycosaminoglycan-bearing polypeptide. Biochem J 1992;288: 565–9
11. Charbonnier F, Périn JP, Mattei MG, et al. Genomic organization of the human SPOCK gene and its chromosomal localization to 5q31. Genomics 1998;48:377–80
12. Alliel PM, Perin JP, Jollès P, et al. Testican, a multidomain testicular proteoglycan resembling modulators of cell social behaviour. Eur J Biochem 1993;214:347–50
13. Marr HS, Basalamah MA, Edgell CJ. Endothelial cell expression of Testican mRNA. Endothelium 1997;5:209–19
14. Marr HS, Basalamah MA, Bouldin TW, et al. Distribution of Testican expression in human brain. Cell Tissue Res 2000;302:139–44
15. Iseki K, Hagino S, Zhang Y, et al. Altered expression pattern of Testican-1 mRNA after brain injury. Biomed Res 2011;32:373–8
16. Schechter I, Ziv E. Cathepsins S, B and L with aminopeptidases display β-secretase activity associated with the pathogenesis of Alzheimer's disease. Biol Chem 2011;392:555–69
17. Merlo S, Sortino MA. Estrogen activates matrix metalloproteinases-2 and -9 to increase amyloid degradation. Mol Cell Neurosci 2012;49: 423–9
18. McLaurin J, Franklin T, Zhang X, et al. Interactions of Alzheimer amyloid-beta peptides with glycosaminoglycans effects on fibril nucleation and growth. Eur J Biochem 1999;266:1101–10
19. McKhann G, Drachman D, Folstein M, et al. Clinical diagnosis of Alzheimer's disease: report of the NINCDS-ADRDA Work Group under the auspices of Department of Health and Human Services Task Force on Alzheimer's Disease. Neurology 1984;34:939–44
20. Clinical and neuropathological criteria for frontotemporal dementia. The Lund and Manchester Groups. J Neurol Neurosurg Psychiatry 1994;57: 416–8
21. Kellner A, Matschke J, Bernreuther C, et al. Autoantibodies against beta-amyloid are common in Alzheimer's disease and help control plaque burden. Ann Neurol 2009;65:24–31
22. Decramer S, Wittke S, Mischak H, et al. Predicting the clinical outcome of congenital unilateral ureteropelvic junction obstruction in newborn by urinary proteome analysis. Nat Med 2006;12:398–400
23. Theodorescu D, Wittke S, Ross MM, et al. Discovery and validation of new protein biomarkers for urothelial cancer: a prospective analysis. Lancet Oncol 2006;7:230–40
24. Theodorescu D, Schiffer E, Bauer HW, et al. Discovery and validation of urinary biomarkers for prostate cancer. Proteomics Clin Appl 2008;2: 556–70
25. Weissinger EM, Wittke S, Kaiser T, et al. Proteomic patterns established with capillary electrophoresis and mass spectrometry for diagnostic purposes. Kidney Int 2004;65:2426–34
26. Deo AK, Borson S, Link JM, et al. Activity of P-Glycoprotein, a β-Amyloid Transporter at the Blood-Brain Barrier, Is Compromised in Patients with Mild Alzheimer Disease. J Nucl Med 2014;55:1106–11
27. Koo EH, Squazzo SL. Evidence that production and release of amyloid beta-protein involves the endocytic pathway. J Biol Chem 1994;269: 17386–9
28. Thinakaran G, Teplow DB, Siman R, et al. Metabolism of the "Swedish" amyloid precursor protein variant in neuro2a (N2a) cells. Evidence that cleavage at the "beta-secretase" site occurs in the golgi apparatus. J Biol Chem 1996;271:9390–7
29. Boland B, Campbell V. A-mediated activation of the apoptotic cascade in cultured cortical neurones: a role for cathepsin-L. Neurobiol Aging 2004;25:83–91
30. Bocock JP, Edgell CJ, Marr HS, et al. Human proteoglycan Testican-1 inhibits the lysosomal cysteine protease cathepsin L. Eur J Biochem 2003;270:4008–15

31. Authier F, Posner BI, Bergeron JJ. Insulin-degrading enzyme. Clin Invest Med 1996;19:149–60
32. Kirschner RJ, Goldberg AL. A high molecular weight metalloendoprotease from the cytosol of mammalian cells. J Biol Chem 1983;258:967–76
33. Misbin RI, Almira EC. Degradation of insulin and insulin-like growth factors by enzyme purified from human erythrocytes. Comparison of degradation products observed with A14- and B26-[125I]monoiodoinsulin. Diabetes 1989;38:152–8
34. Qiu WQ, Walsh DM, Ye Z, et al. Insulin-degrading enzyme regulates extracellular levels of amyloid beta-protein by degradation. J Biol Chem 1998;273:32730–8
35. Edgell CJ, BaSalamah MA, Marr HS. Testican-1: a differentially expressed proteoglycan with protease inhibiting activities. Int Rev Cytol 2004;236:101–22
36. Cui H, Freeman C, Jacobson GA, et al. Proteoglycans in the central nervous system: role in development, neural repair, and Alzheimer's disease. IUBMB Life 2013;65:108–20
37. Fraser PE, Nguyen JT, Chin DT, et al. Effects of sulfate ions on Alzheimer beta/A4 peptide assemblies: implications for amyloid fibril-proteoglycan interactions. J Neurochem 1992;59:1531–40
38. Cohlberg JA, Li J, Uversky VN, et al. Heparin and other glycosaminoglycans stimulate the formation of amyloid fibrils from alpha-synuclein in vitro. Biochemistry 2002;41:1502–11
39. Ariga T, Miyatake T, Yu RK. Role of proteoglycans and glycosaminoglycans in the pathogenesis of Alzheimer's disease and related disorders: amyloidogenesis and therapeutic strategies–a review. J Neurosci Res 2010;88:2303–15
40. Bruinsma IB, te Riet L, Gevers T, et al. Sulfation of heparan sulfate associated with amyloid-beta plaques in patients with Alzheimer's disease. Acta Neuropathol 2010;119:211–20
41. van Horssen J, Otte-Höller I, David G, et al. Heparan sulfate proteoglycan expression in cerebrovascular amyloid beta deposits in Alzheimer's disease and hereditary cerebral hemorrhage with amyloidosis (Dutch) brains. Acta Neuropathol 2001;102:604–14
42. Morawski M, Brückner G, Jäger C, et al. Involvement of perineuronal and perisynaptic extracellular matrix in Alzheimer's disease neuropathology. Brain Pathol 2012;22:547–61
43. Fawcett JW. The extracellular matrix in plasticity and regeneration after CNS injury and neurodegenerative disease. Prog Brain Res 2015;218:213–26
44. Kang J, Lemaire HG, Unterbeck A, et al. The precursor of Alzheimer's disease amyloid A4 protein resembles a cell-surface receptor. Nature 1987;325:733–6
45. Burg MA, Cole GJ. Claustrin, an antiadhesive neural keratan sulfate proteoglycan, is structurally related to MAP1B. J Neurobiol 1994;25:1–22
46. Zimmermann DR, Ruoslahti E. Multiple domains of the large fibroblast proteoglycan, versican. Embo J 1989;8:2975–81
47. Yamada H, Watanabe K, Shimonaka M, et al. Molecular cloning of brevican, a novel brain proteoglycan of the aggrecan/versican family. J Biol Chem 1994;269:10119–26
48. Lein ES, Zhao X, Gage FH. Defining a molecular atlas of the hippocampus using DNA microarrays and high-throughput in situ hybridization. J Neurosci 2004;24:3879–89
49. de Wit J, O'Sullivan ML, Savas JN, et al. Unbiased discovery of glypican as a receptor for LRRTM4 in regulating excitatory synapse development. Neuron 2013;79:696–711
50. Sisodia SS. Beta-amyloid precursor protein cleavage by a membrane-bound protease. Proc Natl Acad Sci U S A 1992;89:6075–9
51. Brunholz S, Sisodia S, Lorenzo A, et al. Axonal transport of APP and the spatial regulation of APP cleavage and function in neuronal cells. Exp Brain Res 2012;217:353–64
52. Cirrito JR, Kang JE, Lee J, et al. Endocytosis is required for synaptic activity-dependent release of amyloid-beta in vivo. Neuron 2008;58:42–51
53. Haass C, Lemere CA, Capell A, et al. The Swedish mutation causes early-onset Alzheimer's disease by beta-secretase cleavage within the secretory pathway. Nat Med 1995;1:1291–6